physical sciences forum

MDPI

Reconstruction, Analysis and Constraints of Cosmological Scalar Field ϕCDM Models †

Olga Avsajanishvili [1,*], **Lado Samushia** [1,2], **Yiwen Huang** [3], **Tina Kahniashvili** [1,4,5,6]

1 E. Kharadze Georgian Nationa and Astrophysical Observatory, Tbilisi 0179, Georgia

2 Department of Physics, Kansas State University, 116 Cardwell Hall, Manhattan, KS, 66506, USA

3 Department of Physics, University of California, San Diego, La Jolla, CA 92093, USA

4 McWilliams Center for Cosmology and Department of Physics, Carnegie Mellon University, 5000 Forbes Ave, Pittsburgh, PA 15213 USA

5 School of Natural Sciences and Medicine, Ilia State University, 3/5 Cholokashvili Ave., Tbilisi 0162, Georgia

6 Department of Physics, Laurentian, University, Ramsey Lake Road, Sudbury, ON P3E 2C, Canada

* Correspondence: olga.avsajanishvili@iliauni.edu.ge

† Presented at the 2nd Electronic Conference on Universe, 16 February–2 March 2023; Available online: https://ecu2023.sciforum.net/.

Abstract: We studied scalar field ϕCDM models: ten quintessence models and seven phantom models. We reconstructed these models, using the phenomenological method developed by us. Resulting in, for each potential the following ranges were found: (i) model parameters; (ii) EoS parameters; (iii) initial conditions for differential equations, which describe the dynamics of the universe. Using the MCMC analysis, we obtained constraints on scalar field models by comparing observations for: the expansion rate of the universe, the angular diameter distance and the growth rate function with corresponding data generated for the fiducial ΛCDM model. We applied the Bayes statistical criteria to compare scalar field models. To this end, we calculated the Bayes factor, as well as the *AIC* and *BIC* information criteria. The results of this analysis showed that we could not uniquely identify the preferable scalar field ϕCDM models compared to the fiducial ΛCDM model based on the predicted DESI data, and that the ΛCDM model is a true dark energy model. We investigated scalar field ϕCDM models in the w_0 - w_a phase space of CPL- ΛCDM contours. We identified subclasses of quintessence and phantom scalar field models, which at the present epoch: (i) can be distinguished from the ΛCDM model; (ii) cannot be distinguished from the ΛCDM model; (iii) can be either distinguished or undistinguished from the ΛCDM model. We found that all studied models can be divided into two classes: models that have attractor solutions and models whose evolution depends on initial conditions.

Keywords: dark energy; scalar field; large-scale structure; Bayesian statistics; Monte Carlo Markov Chains analysis

Citation: Avsajanishvili, O.; Samushia, L.; Huang, Y.; Kahniashvili, T. Reconstruction, analysis and constraints of cosmological scalar field ϕ CDM models. *Phys. Sci. Forum* **2023**, *3*, x. https://doi.org/10.3390/xxxxx

Published: 18 February 2023

1. Introduction:

According to measurements of the Supernovae type Ia magnitudes, our universe is expanding with an acceleration [1, 2]. One of the possible explanations of this fact is that the energy density of the universe is dominated by so-called *dark energy*, a component with effective negative pressure [3]. The simplest description of dark energy is the concept of vacuum energy or cosmological constant Λ [4]. The energy density of the cosmological constant does not depend on time and has recently become dominant (in particular, the energy density associated with the cosmological constant is about 69% of the total energy density of the universe at present epoch [5]). Sometimes the ΛCDM model is referred as a standard, fiducial model. The theoretical predictions of the ΛCDM model are in good

agreement with current observations, but there are several unresolved problems associated with this model [6].

The main alternatives to the ΛCDM model of dark energy are dynamical *scalar field* models, in which energy density depends on time [7, 8]. In these models, a spatially uniform cosmological scalar field, slowly rolling down its almost flat self-interaction potential, plays a role of time-dependent cosmological constant Λ. In scalar field models, the equation of state (EoS) parameter w_ϕ depends on time: $w_\phi \equiv p_\phi/\rho_\phi$, where p_ϕ and ρ_ϕ are respectively, the pressure and density energy of the scalar field; whereas in the ΛCDM model, the EoS parameter is a constant, $w_\Lambda = -1$. Depending on the value of the EoS parameter, ϕCDM scalar field models are divided into: quintessence models, with $w_\phi \in (-1; -1/3)$ [9], and phantom models, with $w_\phi < -1$ [10]. Quintessence models are divided into two classes: tracker (freezing) models, in which the scalar field evolves slower than the Hubble expansion rate, and thawing models, in which the scalar field evolves faster than the Hubble expansion rate [11].

We studied a number of the ϕCDM scalar field models in order to determine the preferred dark energy models compared to the ΛCDM model at the present epoch using the predicted data for the Dark Energy Spectroscopic Instrument (DESI) observations [12, 13]. For this purpose, we carried out the statistical Bayesian analysis, such as Bayes coefficients, as well as Akaike and Bayesian information criteria. We found that the results of the Bayesian analysis provide compelling evidence in favor of the ΛCDM model. We also conducted the Monte Carlo Markov Chains (MCMC) analysis and obtained the constraints on the parameters of the scalar field models, comparing the observational data for: the universe expansion rate of the universe, the angular diameter distance and the growth rate function, with the corresponding data generated for the ΛCDM model.

We investigated how well the Chevallier-Polarsky-Linder (CPL) parametrization approximates the various scalar field models. We determined the location of the scalar field model in the phase space of the CPL parameter. In this manuscript, we used the natural system of units: $c = k_B = 1$.

2. Methods

We considered two types of scalar field ϕCDM models for the spatially flat universe: the quintessence and the phantom scalar field ϕCDM models. We assumed that the flat, homogeneous and isotropic universe is described by the Friedmann– Lemaître–Robertson–Walker spacetime metric, $ds^2 = dt^2 - a^2(t)d\boldsymbol{x}^2$, here $a(t)$ is the scale factor (normalized to be unity at present epoch $a_0 \equiv a(t_0)$), and t is the cosmic time.

The action and the equation of motion of the Klein–Gordon scalar field for the scalar field are, respectively

$$S = \frac{M_{pl}^2}{16\pi}\int d^4x\,[\sqrt{-g}(\pm\frac{1}{2}g^{\mu\nu}\,\partial_\mu\phi\partial_\nu\phi - V(\phi))], \quad (1)$$

$$\ddot{\phi} + 3\frac{\dot{a}}{a} \pm \frac{\partial V(\phi)}{\partial\phi} = 0 \quad (2)$$

where M_{pl} is a Plank mass, " $\pm$ " sign corresponds to the quintessence/phantom model, the over-dot denotes a derivative with respect to the cosmic time, $g^{\mu\nu}$ is the background metric, $V(\phi)$ is the self-interacting potential of the scalar field ϕ.

The energy density ρ_ϕ, pressure p_ϕ and EoS parameter w_ϕ of the scalar field are defined, respectively, as

$$\rho_\phi = \frac{M_{pl}^2}{16\pi}(\pm\dot{\phi}^2/2 + V(\phi)), \quad (3)$$

$$p_\phi = \frac{M_{pl}^2}{16\pi}\left(\pm\dot{\phi}^2/2 - V(\phi)\right), \quad (4)$$

$$w_\phi = \frac{p_\phi}{\rho_\phi} = \frac{\pm\dot{\phi}^2/2 - V(\phi)}{\pm\dot{\phi}^2/2 + V(\phi)} \quad (5)$$

The regime of a slowly rolling scalar field, in which $w_\phi \approx -1$, is realized under the condition that the kinetic term is much less than the potential one, *i.e.*, $|\pm\dot{\phi}^2/2| \ll V(\varphi)$.

The EoS parameter of dark energy models is often represented by the CPL $w_0 - w_a$ parametrization [14, 15]

$$w(a) = w_0 + w_a(1 - a) \quad (6)$$

where $w_0 = w(a = 1)$ and $w_a = -a^{-2}\left(\frac{dw}{da}\right)|_{a=1/2}$. The CPL parametrization of the EoS parameter for the standard ΛCDM model has the form: $(w_0, w_a) = (-1, 0)$.

We studied seven phantom and ten quintessence scalar field φCDM models with corresponding potentials:

The quintessence models

- Ratra–Peebles potential: $V(\phi) = V_0 M_{pl}^2 \phi^{-\alpha}, \alpha = const > 0$ [7]
- Ferreira–Joyce potential: $V(\phi) = V_0\, exp\left(-\lambda\phi/M_{pl}\right), \lambda = const > 0$ [16]
- Zlatev–Wang–Steinhardt potential: $V(\phi) = V_0(exp(M_{pl}/\phi) - 1)$ [17]
- Sugra potential: $V(\phi) = V_0\varphi\phi^{-\chi}\, exp\left(\gamma\phi^2/M_{pl}^2\right), \chi, \gamma = const > 0$ [18]
- Sahni–Wang potential: $V(\phi) = V_0(\cosh(\varsigma\phi) - 1)^g, \varsigma = const > 0, g = const < 1/2$ [19]
- Barreiro–Copeland–Nunes potential: $V(\phi) = V_0(exp(\nu\phi) + exp(\upsilon\phi)); \nu, \upsilon = const \geq 0$ [20]
- Albrecht–Skordis potential: $V(\phi) = V_0((\phi - B)^2 + A)exp(-\mu\phi), A, B = const \geq 0, \mu = const > 0$ [21]
- Urena–Lopez–Matos potential: $V(\phi) = V_0 sinh^m\left(\xi M_{pl}\phi\right), \xi = const > 0, m = const < 0$ [22]
- Inverse exponent potential: $V(\phi) = V_0 exp(M_{pl}/\phi)$ [23]
- Chang–Scherrer potential: $V(\phi) = V_0\left(1 + exp(-\tau\phi)\right), \tau = const > 0$ [24]

The phantom models

- Fifth power potential: $V(\phi) = V_0\phi^5$ [25]
- Inverse square potential: $V(\phi) = V_0\phi^{-2}$ [25]
- Exponent potential: $V(\phi) = V_0\, exp(\beta\phi), \beta = const > 0$ [25]
- Quadratic potential: $V(\phi) = V_0\phi^2$ [26]
- Gaussian potential: $V(\phi) = V_0(1 - exp(\phi^2/\sigma^2)); \sigma = const$ [26]
- Pseudo Nambu-Goldstone boson potential: $V(\varphi) = V_0(1 - cos(\phi/k)), \kappa = const > 0$ [27]
- Inverse hyperbolic cosine potential: $V(\phi) = V_0\,(cosh(\psi\phi))^{-1}, \psi = const > 0$ [28]

We carried out the MCMC analysis to answer the question: "Is it possible to determine the preferred scalar field ϕCDM models compared to the ΛCDM model at present epoch using the predicted data from DESI observations [29]?"

The MCMC analysis based on calculated theoretical model predictions values of:

- **The normalized Hubble parameter for the spatially flat universe**:

$$E(z) = H(z)/H_0 = (\Omega_{r0}(1+z)^4 + \Omega_{m0}(1+z)^3 + \Omega_{\varphi}(z))^{1/2} \quad (7)$$

here $z = 1/a - 1$ is a redshift, $H(z) = \dot{a}/a$ is a Hubble parameter; H_0 is a Hubble constant; Ω_{r0}, Ω_{m0} and Ω_{ϕ} are density parameters at present epoch for radiation, matter and scalar field, respectively.

• The angular diameter distance for the spatially flat universe:

$$d_A(z) = \frac{1}{H_0\,(1+z)} \int_0^z \frac{dz'}{E(z')} \quad (8)$$

• The combination of the growth rate of the matter density fluctuations and the matter power spectrum amplitude $f(a)\sigma_8(a)$ for each ϕCDM model and ΛCDM one.

The growth rate of the matter density fluctuations is given as: $f(a) = dlnD(a)/dlna$, here $D(a) = \delta(a)/\delta(a_0)$ is the linear growth factor representing the normalized matter density fluctuations $\delta(a)$ per the value of those at present epoch $\delta(a_0)$. The linear growth factor is evaluated by solving the linear perturbation equation [30]

,

$$D'' + \left(\frac{3}{a} + \frac{E'}{E}\right)D' - \frac{3\Omega_{m0}}{2a^5E^2}D = 0 \quad (9)$$

where a prime denotes a derivative with respect to the scale factor.

The growth rate of matter density fluctuations $f(a)$ can be parameterized as $f(a) \approx [\Omega_m(a)]^{\gamma(a)}$ [31],

where $\Omega_m(a) = \Omega_{m0}a^{-3}/E^2(a)$ is a fractional matter density; $\gamma(a)$ is the growth index, which in general is a time-dependent function.

The growth index $\gamma(a)$ can be parameterized by a scale factor independent manner, so called the Linder γ - parametrization [32]

$$\gamma = \begin{cases} 0.55 + 0.05(1 + w0 + 0.5wa), & \text{if } w_0 \geq -1; \\ 0.55 + 0.02(1 + w0 + 0.5wa), & \text{if } w_0 < -1. \end{cases} \quad (10)$$

The value of the γ depends on the characteristics (EoS parameter) of the dark energy model being equal to 0.55 for the ΛCDM model [33].

The matter power spectrum amplitude $\sigma_8(a) = D(a)\sigma_8$, here $\sigma_8 = \sigma_8(a_0)$ is the rms linear fluctuation in the mass distribution on scales $8h^{-1}Mpc$, h is a dimensionless normalized Hubble constant, $H_0 = 100h\ km\ c^{-1}Mpc^{-1}$. We applied the value of $\sigma_8 = 0.815$ obtained by Plank 2015 mission [33].

• Our variances correspond to the predicted variances for DESI observations in the redshift range $z \in (0.15; 1.85)$

To obtain the starting points for MCMC analysis, for each quintessence and phantom model, we jointly integrated the Klein-Gordon scalar field equation of motion Eq. (2), the Eq. (7), and the linear perturbation equation Eq. (9), for a wide range of model parameters and the initial conditions. For each potential, plausible solutions were found, for which the following three criteria had to be fulfilled simultaneously:

1. The transition between the matter and dark energy equality ($\Omega_m = \Omega_{\varphi}$) happens relatively recently $z \in (0.6;\ 0.8)$;

2. The growth rate of the matter density fluctuations $f(a)$ and fractional matter density $\Omega_m(a)$ are parameterized by the Linder γ-parametrization Eq. (10);

3. The EoS parameter predicted by the different dark energy models should be in the agreement with the expected EoS parameter value at present epoch (for phantom models

$w_0 < -1$; for the quintessence models with $w_0 \in (-1; -0.75)$, taking into account that for the freezing type $w_a < 0$ and for the thawing type $w_a > 0$).

In the result of the MCMC analysis, for each potential, a posteriori ranges of model parameters and initial conditions were obtained, which included the prior ranges of initial conditions and model parameters. We calculated the covariance matrix of $d_A(z)$, $E(z)$, and $f(z)\sigma_8(z)$ measurements following the standard Fisher matrix approach described in Ref. [29]. We assumed 14 000 sq. deg. of sky coverage and wavenumbers up to $k_{max} = 0.2\ Mpc/h$. We also took into account for covariance between measurements within the same redshift bin: $d_A(z)$, and $E(z)$ measurements are negatively correlated by about 40%, while correlations with $f(z)\sigma_8(z)$ are below 10% for all redshift bins.

To evaluate the quality of various models and distinguish them from each other, we applied the obtained posterior ranges of model parameters and initial conditions to conduct the Bayesian statistics. For this we calculated the Akaike (*AIC*) [34] and Schwarz (*BIC*) [35] information criteria, as well as the Bayes evidence. The *AIC* and *BIC* are defined respectively as

,

$$AIC = -2ln\mathcal{L}_{max} + 2k \tag{11}$$

$$BIC = -2ln\mathcal{L}_{max} + kln \tag{12}$$

where $ln\mathcal{L}_{max} \propto \exp(-\chi^2_{min}/2)$ is the maximum value of the probability function; N is a number of free parameters, k is the number of the observations.

The Bayes evidence for the model with a set of parameters **b** is given by the integral

$$\mathcal{E} = \int d^3\boldsymbol{p}\mathcal{P}(\boldsymbol{p}) \tag{13}$$

where $\mathcal{P}$ is the posterior likelihood, which is proportional to the local density of the MCMC points.

We also investigated how the various scalar field models can be approximated by the CPL parametrization. To this end, we plotted the CPL-ΛCDM 3σ confidence level contours using MCMC technique and displayed on them the largest ranges of the EoS parameters values at present epoch for each ϕCDM model, see Fig. (1). These ranges were obtained for different values of model parameters or initial conditions from the prior ranges.

3. Results and Discussion

Applying the phenomenological method developed by us, we reconstructed ten quintessence and seven phantom scalar field ϕCDM models in the spatially flat universe, *i.e.*, we found the prior ranges for initial conditions and free parameters.

The constraints on dark energy models were obtained by comparing $d_A(z)$, $E(z)$, and $f(z)\sigma_8(z)$ data with the corresponding data generated for the fiducial ΛCDM model using the DESI observations.

For each potential, a posteriori ranges of model parameters and initial conditions were obtained, which include the prior ranges of initial conditions and model parameters.

We applied these posterior ranges to conduct the Bayesian statistics. For this aim, we calculated the Akaike and Schwarz information criteria, as well as the Bayes evidence. The calculated values of *AIC* and *BIC* and Bayes factor for all the dark energy models are summarized in Table 1 and in Table 2. These numbers clearly demonstrated that if the ΛCDM model is the true description of dark energy, then the full DESI data will be able to strongly discriminate most of the scalar field dark energy models currently under consideration.

Table 1. The list of the scalar field ϕCDM phantom models potentials, ith corresponding *AIC*, *BIC*, and Bayes factors.

Phantom potentials	AIC	BIC	Bayes factor
$V(\phi) = V_0\phi^5$	10	18.7	0.0921
$V(\phi) = V_0\phi^{-2}$	10	18.7	0.0142
$V(\phi) = V_0 \exp(\beta\phi)$	22.4	12	0.0024
$V(\phi) = V_0\phi^2$	10	18.7	0.0808
$V(\phi) = V_0(1 - \exp(\phi^2/\sigma^2))$	12	22.4	0.0113
$V(\phi) = V_0(1 - \cos(\phi/\kappa))$	12	22.4	0.0061
$V(\phi) = V_0(\cosh(\psi\phi))^{-1}$	12	22.4	0.0056

Table 2. The list of the scalar field ϕCDM quintessence models potentials, ith corresponding *AIC*, *BIC*, and Bayes factors.

Quintessence potentials	AIC	BIC	Bayes factor
$V(\phi) = V_0 M_{\rm pl}^2\phi^{-\alpha}$	10	18.7	0.5293
$V(\phi) = V_0 \exp(-\lambda\phi/M_{\rm pl})$	12	22.4	0.0059
$V(\phi) = V_0(\exp(M_{\rm pl}/\phi) - 1)$	10	18.7	0.0067
$V(\phi) = V_0\phi^{-\chi} \exp(\gamma\phi^2/M_{\rm pl}^2)$	14	26.2	0.0016
$V(\phi) = V_0(\cosh(\varsigma\phi) - 1)^g$	14	26.2	0.0012
$V(\phi) = V_0(\exp(\nu\phi) + \exp(\upsilon\phi))$	14	26.2	0.0053
$V(\phi) = V_0((\phi - B)^2 + A)\exp(-\mu\phi)$	16	29.9	0.0034
$V(\phi) = V_0 \sinh^m(\xi M_{\rm pl}\phi)$	14	26.2	0.0014
$V(\phi) = V_0 \exp(M_{\rm pl}/\phi)$	10	18.7	0.0077
$V(\phi) = V_0(1 + \exp(-\tau\phi))$	12	22.4	0.0024

We investigated how the dark energy models are mapped on the $w_0 - w_a$ phase space of the CPL - ΛCDM contours, see Fig. (1).

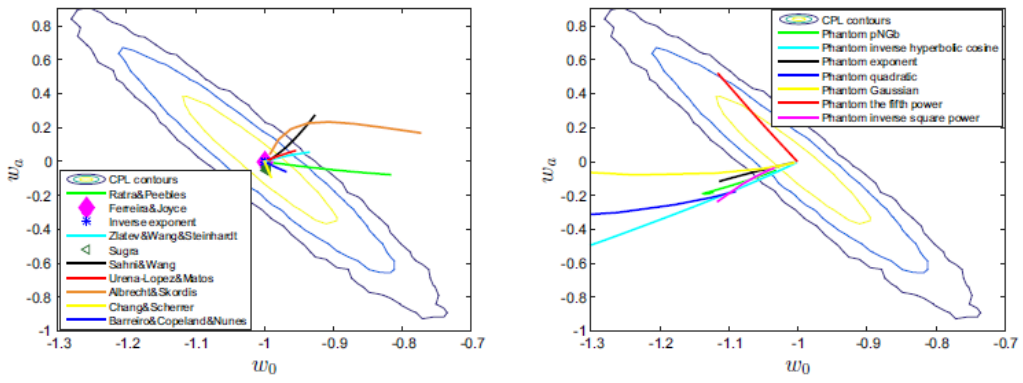

Figure 1. The comparison of the possible (w_0, w_a) values of the quintessence (left panel) and phantom (right panel) scalar field potentials with the CPL-ΛCDM 3σ confidence level contours.

We found that quintessence models: the Ferreira-Joyce, the inverse exponent, the Sugra, the Chang-Scherrer, the Urena-Lopez-Matos, the Barreiro-Copeland-Nunes and the fifth power phantom model cannot be distinguished from the ΛCDM model at present epoch. Whilst quintessence models: the Ratra-Peebles, the Zlatev-Wang-Steinhardt, the Albrecht-Skordis, the Sahni-Wang and phantom models: the pseudo-Nambu-Goldstone boson, the inverse hyperbolic cosine, the exponent, the Gaussian, the inverse square power can either be distinguished or cannot be distinguished from the ΛCDM model at present epoch. The phantom quadratic model can be absolutely distinguished from the ΛCDM model at the present epoch.

All the studied models can be divided into two types: models whose evolution depends on the values of the initial conditions and into models whose evolution doesn't depend on values of the initial conditions. The first type includes the following quintessence models: the Zlatev-Wang-Steinhardt, the Sahni-Wang and also the phantom models: the quadratic, the Gaussian, the fifth power, the inverse square power. The second type includes the following quintessence models: the Sugra, the Chang-Scherrer, the Albrecht-Skordis, the Urena-Lopez-Matos, the Barreiro Copeland-Nunes, as well as the following phantom models: the pseudo-Nambu-Goldstone boson, the inverse hyperbolic cosine, the exponent.

4. Conclusions

We investigated ten quintessence and seven phantom scalar field ϕCDM models in the spatially flat universe. We reconstructed these models using the phenomenological method developed by us.

We carried out constraints of scalar field ϕCDM models by the predicted DESI data applying the MCMC analysis. These constraints were obtained by comparing the normalized Hubble parameter $E(z)$, the angular diameter distance $d_A(z)$, the combination of the growth rate of the matter density fluctuations and the matter power spectrum amplitude $f(a)\sigma_8(a)$ data with the corresponding data generated for the fiducial ΛCDM model.

We applied the Bayes statistical criteria to compare the models, such as the Bayes factor, as well as the *AIC* and *BIC* information criteria. Using the Bayesian statistical analysis, we could not uniquely identify preferable ϕCDM models compared to the fiducial ΛCDM model based on the predicted DESI data, so the ΛCDM model is a true model.

Mapping ϕCDM models in the phase space of the CPL-ΛCDM contours, we could identify the subclasses of these models, which: i) have the attractor and usual solutions, ii) can be distinguished, iii) cannot be distinguished, iv) can be either distinguished or undistinguished from the ΛCDM model at present epoch.

Acknowledgements Supported by the Shota Rustaveli National Science Foundation grant FR-19-8306.

References

1. A. G. Riess et al., Astron. J. **116,** 1009-1038 (1998).
2. S. Perlmutter et al., Astrophys. J. **517**, 565-586 (1999).
3. J.Frieman, M. Turner and D. Huterer, Ann. Rev. Astron. Astrophys.**46**, 385-432 (2008).
4. A. Einstein, A. Sitzungsber. Preuss. Akad. Wiss. Berlin (Math. Phys.), 778-786 (1915).
5. N. Aghanim et al. (Planck), Astron. Astrophys. **641**, A6 (2020).
6. E. Di Valentino, Universe 8, 399 (2022).
7. B. Ratra, P. J. E. Peebles., Astrophys. J. **325**, L17-L20 (1988).
8. C. Wetterih, Nul. Phys.B302, 645-667 (1988).
9. P. J. E. Peebles and B. Ratra, Rev. Mod. Phys. **75**, 559 (2003).
10. R. R. Caldwell, Phys. Lett. B **545**, 23 (2002).
11. P. H. Frampton, K. J. Ludwick, and R. J. Scherrer, Phys. Rev. D **84**, 063003 (2011).
12. M. Levi et al. [DESI Collaboration] arXiv:1308.0847 (2013).
13. A. Aghamousa et al. [DESI Collaboration] arXiv:1611.00036 (2016).

14. M. Chevallier, D. Polarski, Int. J. Mod. Phys. D **10**, 213 (2001).
15. E.V. Linder, Phys. Rev. Lett. **90**, 091301 (2003).
16. P.G. Ferreira, M. Joyce, Phys. Rev. D **58**, 023503 (1998).
17. I. Zlatev, L.M. Wang, P.J. Steinhardt, Phys. Rev. Lett. **82**, 896 (1999).
18. P. Brax, J. Martin, Phys. Lett. B **468**, 40 (1999).
19. V. Sahni, L.M. Wang, Phys. Rev. D **62**, 103517 (2000).
20. T. Barreiro, E.J. Copeland, N.J. Nunes, Phys. Rev. D **61**, 127301 (2000).
21. A. Albrecht, C. Skordis, Phys. Rev. Lett. **84**, 2076 (2000).
22. L.A. Urena-Lopez, T. Matos, Phys. Rev. D **62**, 081302 (2000).
23. R.R. Caldwell, E.V. Linder, Phys. Rev. Lett. **95**, 141301 (2005).
24. H.Y. Chang, R.J. Scherrer, arXiv:1608.03291 (2016).
25. R.J. Scherrer, A.A. Sen, Phys. Rev. D **78**, 067303 (2008).
26. S. Dutta, R.J. Scherrer, Phys. Lett. B **676**, 12 (2009).
27. J.A. Frieman, C.T. Hill, A. Stebbins, I. Waga, Phys. Rev. Lett. **75**, 2077 (1995).
28. R. Rakhi, K. Indulekha, arXiv:0910.5406 (2009).
29. A. Font-Ribera, P. McDonald, N. Mostek, B.A. Reid, H.J. Seo, A. Slosar, JCAP **1405**, 023 (2014).
30. L.M. Wang, P.J. Steinhardt, Astrophys. J. **508**, 483 (1998).
31. E.V. Linder, R.N. Cahn, Astropart. Phys. **28**, 481 (2007).
32. F. Pace, J.-C. Waizmann, M. Bartelmann, Mon. Not. R. Astron.Soc. **406**, 1865 (2010).
33. P.A.R. Ade et al. [Planck Collaboration], Astron. Astrophys. **594**, A13 (2016).
34. H. Akaike, IEEE Transations on Automatic Control **19**(06), 716-723 (1974).
35. G.H. Schwarz, Annals of Statistics, **06**(02), 461-464 (1978).